Thermokarst Lake Eccentricity in Alaska's Eastern Arctic Coastal Plain

Rowan Biessel

***Abstract*—Thermokarst lakes are a dominant feature of northern permafrost environments. In regions like the Alaskan Arctic Coastal Plain (ACP) as well as parts of the Arctic and on the Tibettan Plateau, many of these lakes have striking ellipsoidal shapes with major axes aligned in a particular direction. In the western part of the ACP, this orientation is in a NNW direction, orthogonal to the prevailing winds. However, This phenomeon has not been well documented on the Eastern Arctic Coastal Plain. I use Sentinel-2 imagery to identify thermokarst lakes and quantify their eccentricity and directionallity at four locations east of and including Prudhoe Bay. Morphometry of the Prudhoe Bay lakes is consistent with that to the west. However, directionality in the other study areas are much more variable but generally follow a NEE orientation rougly parallel to prevailing winds. This is also true south of Prudhoe bay along the Dalton Highway. These differences motivate further study into the mechanisms behind directional thermokarst expansion.**

***Index Terms*—Permafrost, Thermokarst Lakes, Digital Image Processing, Arctic**

I. Introduction

The Alaskan Arctic Coastal Plain (ACP) covers a vast majority of Alaska's North Slope and is characterized by low relief and a high density of thermokarst lakes. Such thermokarst lakes are an expression of the ongoing degradation of ice-rich permafrost in this region. As this ice-rich permafrost degrades, the ground surface subsides, allowing water to pool. Such thermo-karst leads to positive feedback as accumulated water further influences the thermal regime of these soils. Further advancement of such processes and coallescense of multiple of these ponds produce larger and larger bodies of water and also lead to the development of elliptical taliks [1], permannently unfrozen ground.

Consequently, thermokarst lakes are a principal driver of permafrost related carbon remobilization [2, 3]. In particular, they provide an apt aneoribic environment for microbial production of methane, a greenhouse gas more potent than CO_2 [4, 5]. Thermokarst also represent prominent habitats for aqautic flora and fauna [6] and also may significantly influence the energy balance of the landscape [7]. Understanding the drivers of thermokarst is an important means of understanding how the arctic is evolving and how it will continue to change in a warming climate.

Thermokarst is generally characterized by gradual thermal erosion and collapse of the shores. This can also happen more suddenly and irregularly due to retrogressive thaw slumping of the surrounding slopes. The highly eccentric morphometry described on the western ACP (WACP), requires that these different thermokarst processes are preferentially active in a dominant direction. The principal explanation for this phenomeon is the prevailing summer wind directions [8, 9].

In the case of the WACP, lake directionality is primarily orthogonal to the prevailing wind, which [8, 9] have attributed to wave action and currents induced in this orthogonal direction as well as due to protection by littoral shelves normal to the wind direction. Similarly, [10] relates this preferential expansion to gyre currents. However, on the Tibettan Plateau, thermokarst lakes have also been observed oriented parallel to the prevailing wind direction [11]. There are a number of differences between these two regions but its unclear what can account for this stark difference in orientation regimes.

Thermokarst lakes are prevelant on the Eastern ACP (EACP) as well, yet they have not been as thoroughly documented as the WACP. Initial inspection of these lakes also suggest that they may not follow the same patterns as those in the WACP. In this study I will quantify thermokarst morphometry in this region using satellite imagery and relate these observations to those of the WACP.

II. Methodology

A. Data & Study Area

I focus this study on four ares of interest (AOIs) within the Eastern ACP (EACP) (Fig. 1). First, the Prudhoe Bay AOI offers a baseline comparison for the WACP. To guage whether the morphometry of these lakes change to the south, I also choose an AOI along the northern part of the Dalton Highway, just south of the Prudhoe bay AOI. I also selected AOIs in the Canning River Delta near Kaktovik in the Arctic National Wildlife Refuge. These are locations of relatively dense lake cover, which is less common east of Prudhoe.

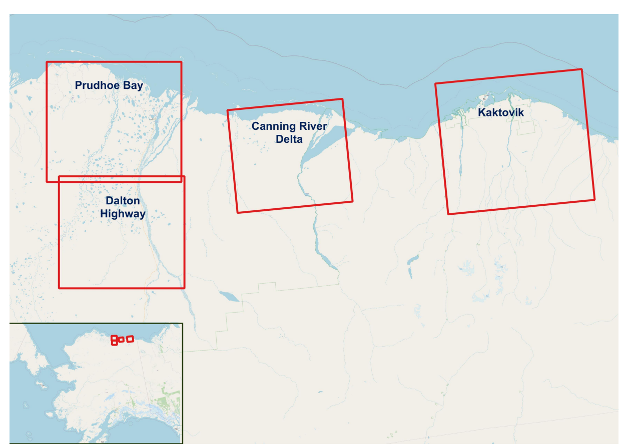

Fig. 1. A map of Alaska's Eastern Arctic Coastal Plain showing the four areas of interest.

To perform this study and the workflow outlined in Fig. 2, I used three cloud-free Sentinel-2 Infrared (band 8) acquired in

2019 and 2020. A variety of platforms could have worked in theory but Sentinel-2 has the advantage of having 10m resolution and frequent enough acquisitions to capture the limited scenarios when these northern regions are not covered by clouds. Near-infrared also has the advantage over other spectra due to its high degree of scattering from tundra/vegetation and very low reflectance in water due to its absorption. This data also lacks the speckle associated with SAR imagery. In light of these factors, a single scene for each study area is sufficient to segment lakes and waterbodies.

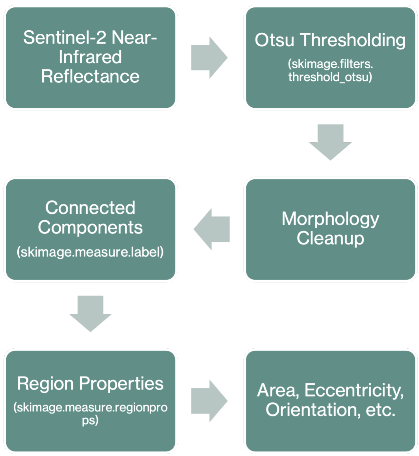

Fig. 2. Flowchart of image processing workflow.

B. Thresholding

I used Otsu's method [12] to automatically select a threshold suitable for segmenting the waterbodies in these scenes. This method is a minimization of within-class variance in which an optimal threshold value is computed iteratively. In other words, the variance between the water bodies and the surrounding tundra is maximized. The contrasts between water bodies and tundra in infrared data makes the Otsu method ideal and convenient. I leveraged the implementation of this algorithm in Scikit-Image ($skimage.filters.threshold\_otsu$), a ubiquitous package for image/data processing in python [13]

An immediate shortfall of this approach is that it is unable to differentiate lakes from other waterbodies like rivers which will also be highly oriented. Other dark features like cloud shadows may also potentially produce false-positives. I found reducing the threshold by a factor of two reduced the classification of creeks, rivers, as well as one cloud shadow. This comes at the cost of excluding the smallest thermokarst ponds. I also applied a morphological opening to further reduce the impact of highly thin creeks and spuriously small regions. For this, I used a 3×3 square structuring element. I did not perform any low-pass filtering on the base imagery.

C. Eccentricity & Directionality

Computing the eccentricity and directionality requires further segmentation of the imagery to separate each unique lake. I did this using a connected components' algorithm implemented in Scikit-Image ($skimage.measure.label$) [13]. This package also provides convenient functionality for computing parameters related to these segmented regions. Using this ($skimage.measure.regionprops$), I computed the area, eccentricity, and directionality of each waterbody. The approach for estimating these parameters is to fit an ellipse to each waterbody based on an analysis of image moments and principal component analysis. The eccentricity is the ratio of the focal length to the major axis length. As the focal length approaches 0, the shape becomes more circular and the eccentricity also approaches 0. On the other hand, highly elliptical lakes will have eccentricities near 1 as the focal length approaches the major axis length. The directionality is simply the angle between the x-axis and the major axis. I converted these to cardinal directions. Finally, the area is the number of pixels multiplied by footprint of each pixel, in this case $100m^2$.

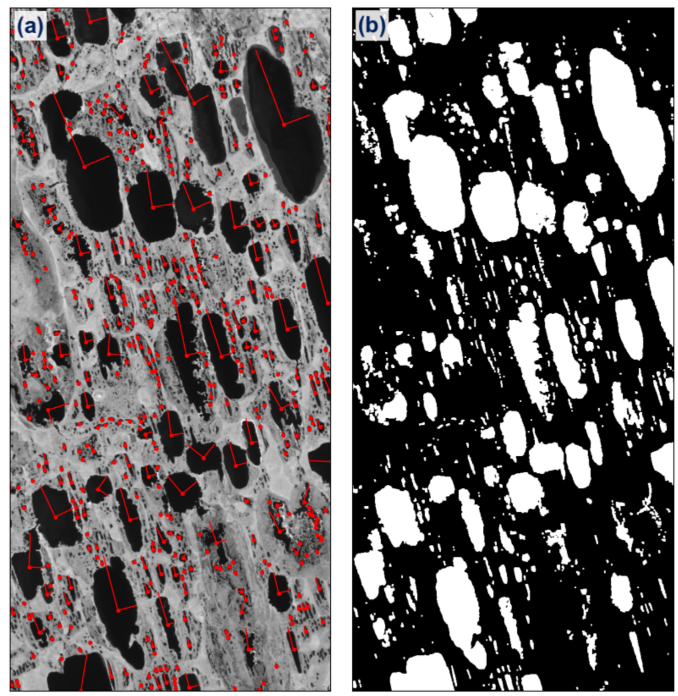

Fig. 3. Two images illustrating outputs of the different processing stages. The image on the left (a) shows an example of the Sentinel-2 reflectance. Overlaid are the centroids of the segmented lakes (dots) and the major and minor axes of the fitted elipsoids as red lines. The image on the right (b) shows the corresponding binary image after a morpholigical opening.

III. Results & Discussion

I plot summary distributions of the ecentricies and lake areas of these regions in 4. I also present Rose diagrams illustrating the distribution of orientations for the four AOIs in Fig. 5. Each of these distributions (except area) are weighted by lake area in order to reduce the bias by river segments. The eccentricity distributions for these four regions didn't diverge too greatly, although the Dalton Highway lakes appears to be more circular than the others.

Orientation distributions are more telling and illustrate a high degree of variability within these four regions. Within the Prudhoe bay AOI, lake directionality was most well aligned and agrees well with the principal orientation of the WACP [9, 8, 10] that is orthogonal to the prevailing SW blowing wind.

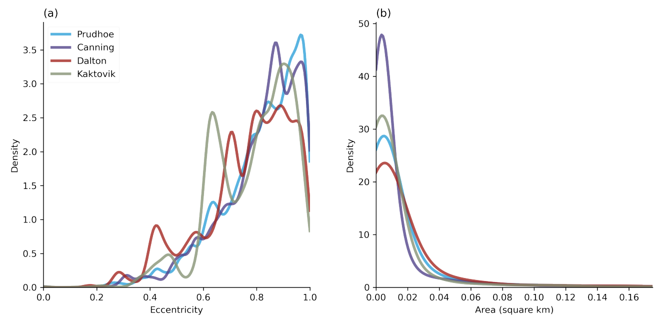

Fig. 4. Distributions of derived eccentricity (a) and lake areas (b) for the four AOIs. Eccentricity distributions are weighted by lake area.

Interestingly, the other regions depart from this pattern. Particularly in the Canning river delta, thermokarst lakes are much more likely to be oriented NEE. This is roughly parallel to the prevailing wind and orthogonal to the orientation of the Prudhoe bay lakes. There still remains a small portion of the lake area here that are oriented in the same NNW direction as near Prudhoe, but these are likely those in the western edge of this AOI near Prudhoe again. The lakes in the Canning River Delta also had the least variability in size and are the smallest out of the four regions studied (Fig. 4).

The Dalton and Kaktovik regions have much more sporadic orientations and eccentricity magnitudes. However, they still appear to have more in common the Canning River AOI than Prudhoe. These two regions generally have the most circular lakes but are still more probable of being oriented in the NEE direction. The consistency of this pattern between the three AOIs suggests this isn't necessarily an artifact of rivers. Round lakes also tend to lie equally in bins that are multiples of $\pi/2$ radians (exactly on N, NE, NW etc.). Although the Kaktovik region has many lakes that lie in the NE direction, much fewer lie in the NE or E bins suggesting it is also not an artifact of low eccentricity. The large peak in the NNW direction in the Kaktovik AOI is likely caused by residual classification of many river segments.

A. Limitations

As previously mentioned, the Otsu thresholding cannot distinguish rivers from lakes. This is also difficult to mitigate via eccentricity as this is a key parameter I'm seeking to quantify with respect to the lakes themselves. There are many thermokarst lakes with highly elongated shapes that would be falsely removed. Instead, I weighted my results based on the lake size. The morphological operations in combination tend to break up rivers into frequent but small features. Weighting subsequent distributions by area then dampens their prominence. However, the influence of rivers still introduces ambiguity with regard to the variance of the derived lake orientations. Some spurious but small peaks in the derived rose diagrams could be attributed to rivers, like the NNW peak in the Kaktovik orientations. This study could be improved

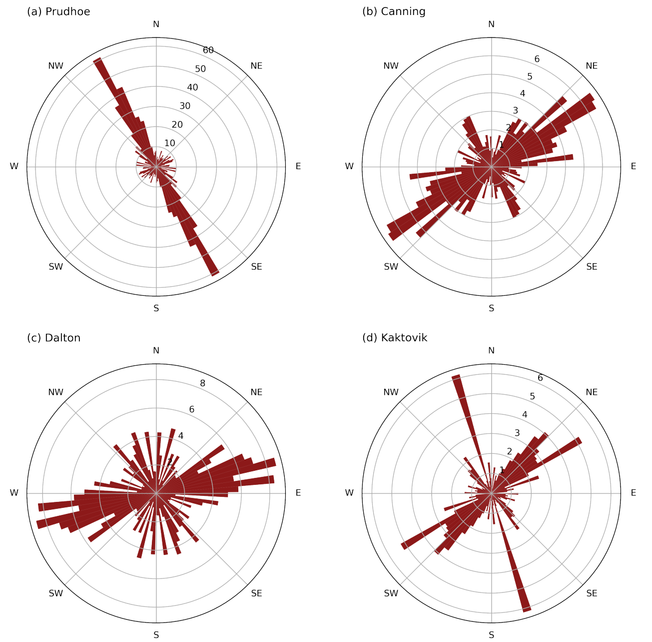

Fig. 5. Rose diagrams of the directionality of thermokarst lakes for each of the four AOIs. Density distributions are weighted by lake area in km^2.

by completely removing lake bodies via a more advanced segmentation approach like deep learning.

Mergers of multiple elongated thermokarst lakes may also impact the results. This can have either the effect of dampening the eccentricity or greatly ehancing it. The former is more likely to also influence the directionality estimates. I do not directly account for this in this study. Rather I treat this occurence as a natural development of these systems and an inherent source of variance in any directionality analyses that is representative of a dynamic landscape.

B. Differences in Orientation Regimes

My future work will attempt to ingest additional variables in an attempt to explain the difference in orientations between the WACP and EACP quantified here. Explanations could be due to differences in for instance permafrost conditions, geology, bathymetry, topography. Pruhoe bay lakes are also characterized by littoral shelves located along the flanks normal to the prevailing wind. In these other regions where directionality is less strongly oriented in this direction or rather oriented orthogonal to the prevailing wind, these littoral shelves are much less visible and closer analysis may be useful.

IV. Conclusion

Lake morphometry in thermokarst envionments is unique and is characterized by being highly elliptical with preferential orientations. I've quantified these eccentricities and directionalities in four AOIs on the Eastern Arctic Coastal Plain. Prudhoe bay and regions to the west, studied by others, are dominated by lakes oriented in the NNW direction, orthogonal to the ACP's prevailing wind. I find that in the EACP, this characterzation breaks down and lakes are generally oriented in the NEE direction. Thermokarst governs much of the landscape evolution of these arctic regions. Understanding the differences in controls between these two thermokarst regimes will be important clues to elucidating how the arctic will be changing over the course of the next few centuries and how these changes may manifest help inform carbon/climate models.

References

[1] Noriaki Ohara et al. “A New Stefan Equation to Characterize the Evolution of Thermokarst Lake and Talik Geometry”. In: *The Cryosphere* 16.4 (Apr. 8, 2022), pp. 1247–1264. ISSN: 1994-0416. DOI: 10.5194/tc-16-1247-2022. URL: https://tc.copernicus.org/articles/16/1247/2022/ (visited on 12/13/2022).

[2] T. Schneider von Deimling et al. “Observation-Based Modelling of Permafrost Carbon Fluxes with Accounting for Deep Carbon Deposits and Thermokarst Activity”. In: *Biogeosciences* 12.11 (June 5, 2015), pp. 3469–3488. ISSN: 1726-4189. DOI: 10.5194/bg-12-3469-2015. URL: https://bg.copernicus.org/articles/12/3469/2015/ (visited on 12/13/2022).

[3] E. A.G. Schuur et al. “Climate Change and the Permafrost Carbon Feedback”. In: *Nature 2015 520:7546* 520.7546 (Apr. 9, 2015), pp. 171–179. ISSN: 1476-4687. DOI: 10.1038/nature14338. pmid: 25855454. URL: https://www.nature.com/articles/nature14338 (visited on 04/25/2022).

[4] Alexey R. Desyatkin et al. “CH4 Emission from Different Stages of Thermokarst Formation in Central Yakutia, East Siberia”. In: *Soil Science and Plant Nutrition* 55.4 (Aug. 1, 2009), pp. 558–570. ISSN: 0038-0768. DOI: 10.1111/j.1747-0765.2009.00389.x. URL: https://doi.org/10.1111/j.1747-0765.2009.00389.x (visited on 12/13/2022).

[5] Michiel H. in ’t Zandt, Susanne Liebner, and Cornelia U. Welte. “Roles of Thermokarst Lakes in a Warming World”. In: *Trends in Microbiology* 28.9 (Sept. 1, 2020), pp. 769–779. ISSN: 0966-842X. DOI: 10.1016/j.tim.2020.04.002. URL: https://www.sciencedirect.com/science/article/pii/S0966842X20300913 (visited on 12/13/2022).

[6] Paschale N. Bégin and Warwick F. Vincent. “Permafrost Thaw Lakes and Ponds as Habitats for Abundant Rotifer Populations”. In: *Arctic Science* 3.2 (June 2017), pp. 354–377. DOI: 10.1139/as-2016-0017. URL: https://cdnsciencepub.com/doi/full/10.1139/as-2016-0017 (visited on 12/13/2022).

[7] D. Franz et al. “Lake-Atmosphere Heat Flux Dynamics of a Thermokarst Lake in Arctic Siberia”. In: *Journal of Geophysical Research: Atmospheres* 123.10 (2018), pp. 5222–5239. ISSN: 2169-8996. DOI: 10.1029/2017JD027751. URL: https://onlinelibrary.wiley.com/doi/abs/10.1029/2017JD027751 (visited on 12/13/2022).

[8] Kenneth M. Hinkel et al. “Morphometric and Spatial Analysis of Thaw Lakes and Drained Thaw Lake Basins in the Western Arctic Coastal Plain, Alaska”. In: *Permafrost and Periglacial Processes* 16.4 (Oct. 2005), pp. 327–341. ISSN: 10456740. DOI: 10.1002/PPP.532.

[9] Charles E. Carson and Keith M. Hussey. “The Oriented Lakes of Arctic Alaska”. In: *The Journal of Geology* (July 1, 1962). DOI: 10.1086/626834. URL: https://www.journals.uchicago.edu/doi/10.1086/626834 (visited on 12/14/2022).

[10] Shengan Zhan et al. “Spatio-Temporal Analysis of Gyres in Oriented Lakes on the Arctic Coastal Plain of Northern Alaska Based on Remotely Sensed Images”. In: *Remote Sensing* 6.10 (10 Oct. 2014), pp. 9170–9193. ISSN: 2072-4292. DOI: 10.3390/rs6109170. URL: https://www.mdpi.com/2072-4292/6/10/9170 (visited on 12/14/2022).

[11] Fujun Niu et al. “Morphological Characteristics of Thermokarst Lakes along the Qinghai-Tibet Engineering Corridor”. In: *Arctic, Antarctic, and Alpine Research* 46.4 (2014), pp. 963–974. ISSN: 1523-0430. JSTOR: 24551858.

[12] N. Otsu. “A Threshold Selection Method from Gray-Level Histograms”. In: *IEEE Transactions on Systems, Man, and Cybernetics* 9.1 (Jan. 1979), pp. 62–66. ISSN: 2168-2909. DOI: 10.1109/TSMC.1979.4310076.

[13] Stefan Van der Walt et al. “Scikit-Image: Image Processing in Python”. In: *PeerJ* 2 (2014), e453.